

High Speed Optical Backplane Bus with Modulation and Demodulation Capabilities

Srikanth Natarajan, Ray. T. Chen, Suning Tang and Robert. A. Mayer

Microelectronics Research Center
Department of Electrical and Computer Engineering
University of Texas, Austin, Texas 78712-1084
Tel: 512-471-4349

Abstract

We report in this paper, an one-dimensional(1-D), 1 Gbit/sec, fully integrated 1-to-10 optical planar bus array. The optical bus is made out of a thin glass substrate in conjunction with an 1-D hologram array, integrated on the surface. Based on the dispersion relation, the angular misalignment can be used to determine the wavelength tolerance of the optical bus, which is a representation of its modulation bandwidth. Using the experimental results of the angular tolerance, which is determined to be 0.5° , it can be shown that a wavelength coverage of 42 nm is achievable when this optical bus is used. The corresponding frequency is 7.5 THz.

1.0 Introduction

The capability of optical interconnects to provide high-speed data transfer, has made them an attractive alternative to replace electrical interconnects in communication systems. Increased research interest in optical interconnects is due to many distinct advantages such as high modulation speed, massive fan-out and longer propagation distances [1]. The functional complexities of VLSI circuits, demand a growing need for higher modulation speed, fan-out capability and a high packing density bus array. As a result of this, electrical interconnects will not be sufficient for intra-module and module-to-module levels. If a clock speed of 1 Gb/s is needed in a circuit, electrical interconnects cannot provide a communication distance of more than a few mm to cm [2]. This in turn limits the scale of integration and thus imposes a strict restriction on electrically interconnected systems.

With increase in cycle time and decrease in pulse widths, the bandwidth needed to preserve the rising and falling edges of the signals increases. This necessitates the employment of bulky, expensive, terminated coaxial cables [3]. Another limitation of electrical buses is their clock skew problem. Clock skew increases signal processing time and introduces errors in the outputs of logic gates. The RC time constants of electrical interconnects are slower than modulation/switching times of transistors that constitute the VLSI circuits. Fan-out capabilities are restricted for electrical interconnects due to electromagnetic interference, parasitic capacitance and inductance coupling [5]. This makes it impossible to fully utilize the high speeds of logic gates. Optical buses can help in making use of these high modulation and switching speeds.

In this paper, the modulation bandwidth of a 1-to-10, 1-D optical backplane bus is demonstrated for the first time. Dispersion measurement is conducted to study the modulation bandwidth of the optical backplane bus. Backplane optical surface normal fan-out interconnection is realized using a light guiding glass in conjunction with an array of 1-D holograms.

2.0 Optical Backplane Fan-out Bus Design

The physical layer of an optical bus presented herein, is essentially a thin glass substrate with a set of 1-D holograms integrated on its surface. Dichromated gelatin (DCG) film is spin coated on the surface of

the glass substrate. Using holographic recording techniques, followed by processing the film in alcohol-water solutions, with gradually increasing percentage of alcohol [7], the desired fan-out/fan-in holograms are obtained. The glass substrate functions as the light-guiding medium.

The optical bus consists of two types of holograms. There is an input grating coupler, which is designed to couple the surface normal TEM_{00} laser beam into a substrate guided beam with a particular bouncing angle. The second type of hologram couples an array of substrate guiding beams into a 1-D array of surface-normal fan-out beams [4] with a specific coupling efficiency. Figure 1 is a schematic of how the optical bus can be used as a backplane in VLSI systems.

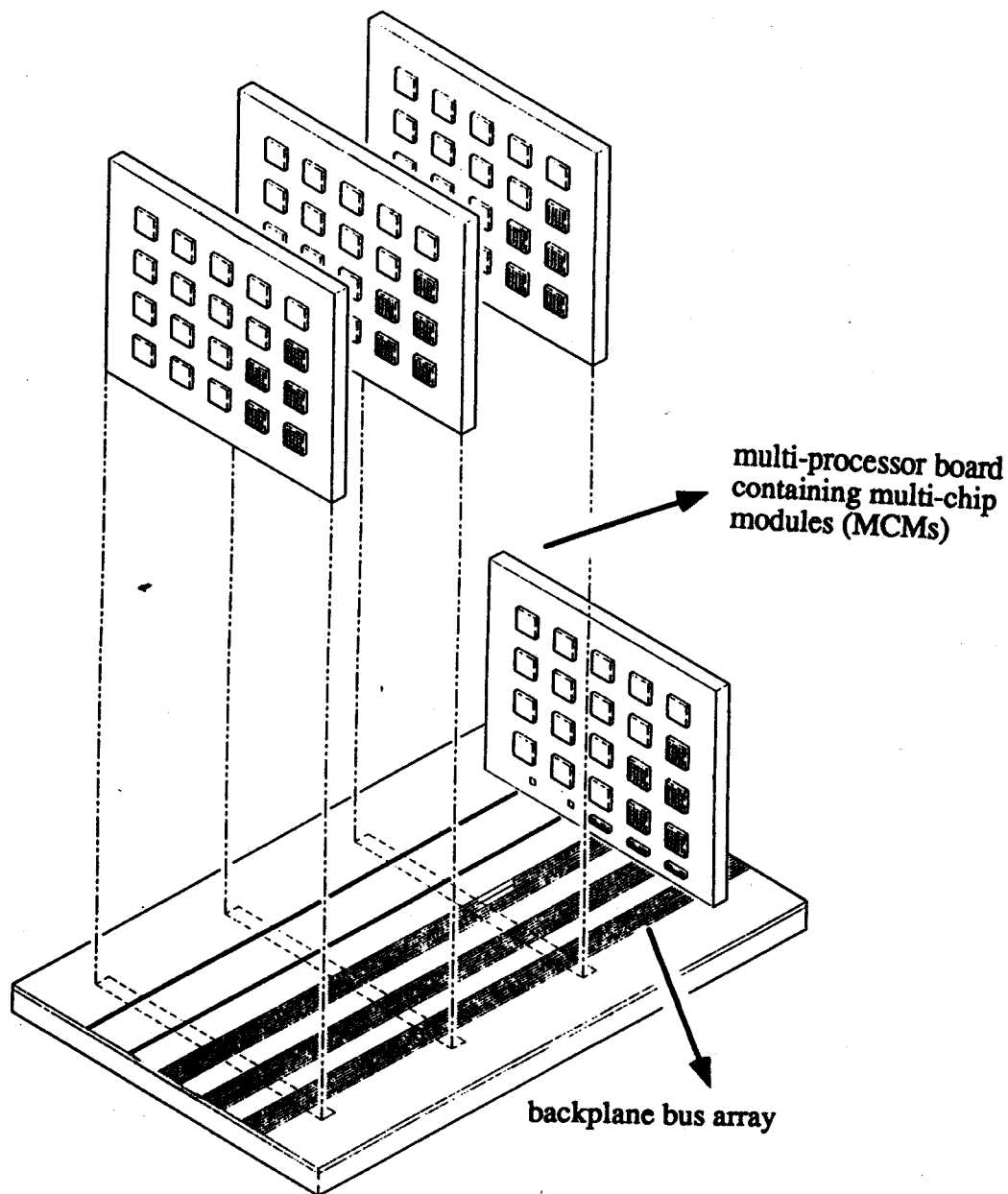


Figure 1. Schematic of the optical backplane bus, with some multichip modules (MCMs).

Figure 2 shows a section of the backplane bus of figure 1. Bi-directional holograms are used to facilitate bi-directional signal flow between the backplane and the multichip modules (MCMs), that are connected to the backplane.

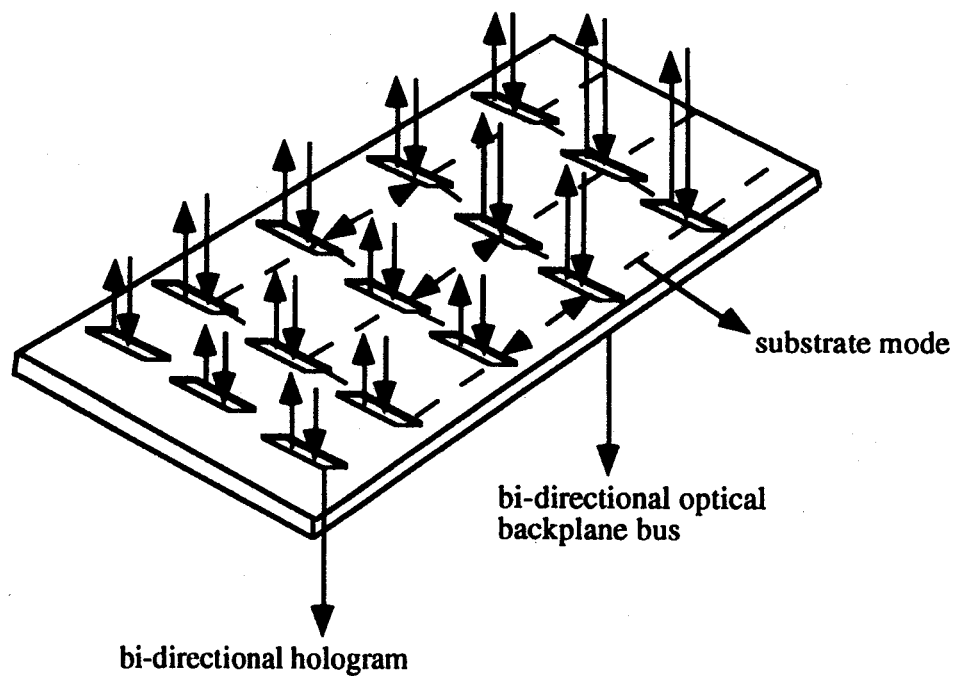


Figure. 2. A section of the optical backplane bus.

3.0 Experimental Results

An integrated linear parallel 1-to-10 surface normal fan-out device working at $1.3 \mu\text{m}$, is fabricated. Its modulation bandwidth is determined, and its functionality in a high-speed transceiver system is demonstrated (figure. 3).

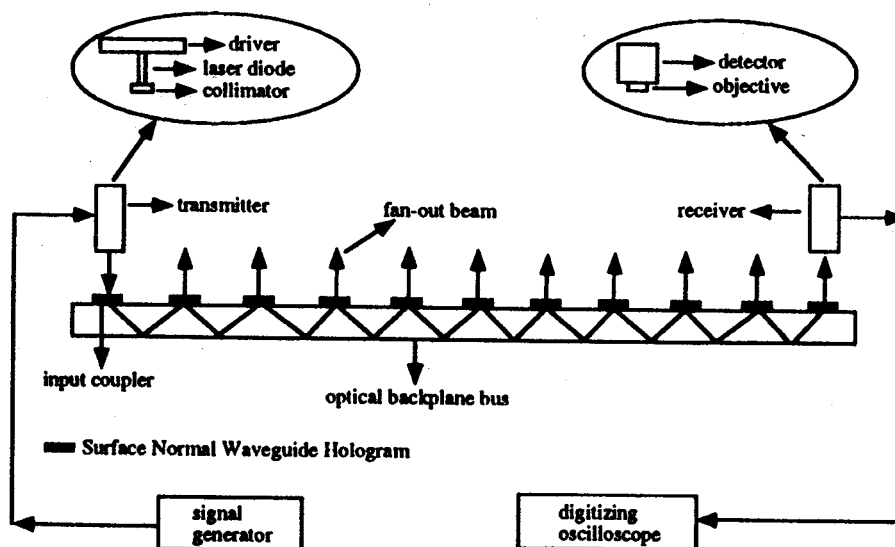


Figure. 3. Experimental setup for the optical backplane bus operating at $1.3 \mu\text{m}$. The modulation frequency is 1 GHz.

A 1 Gbit/sec amplitude modulated semiconductor laser beam at 1300 nm is applied to the device fabricated. This input beam is from a high-speed transmitter. A high-speed receiver is employed to detect the light beam. The sine-shaped 1 GHz modulation signal is provided by an HP 8656B signal generator. Figure 4 is a picture of the 1-to-10 optical fan-out from the bus, at 1.3 μm . The length of the device shown in figure 4 is 5 cm. Figure 5 shows the input and output signals of the optical fan-out interconnect obtained by a Tektronics 11403 Digitizing Oscilloscope.

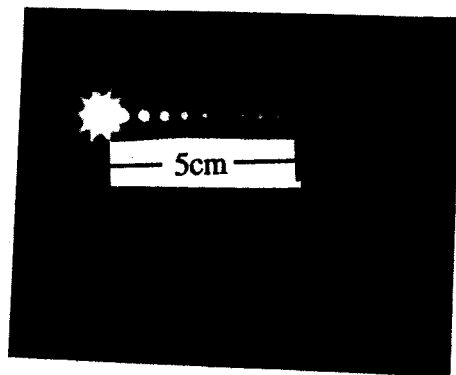


Figure 4. Picture of 1-to-10 fan-out from the optical bus at 1.3 μm .

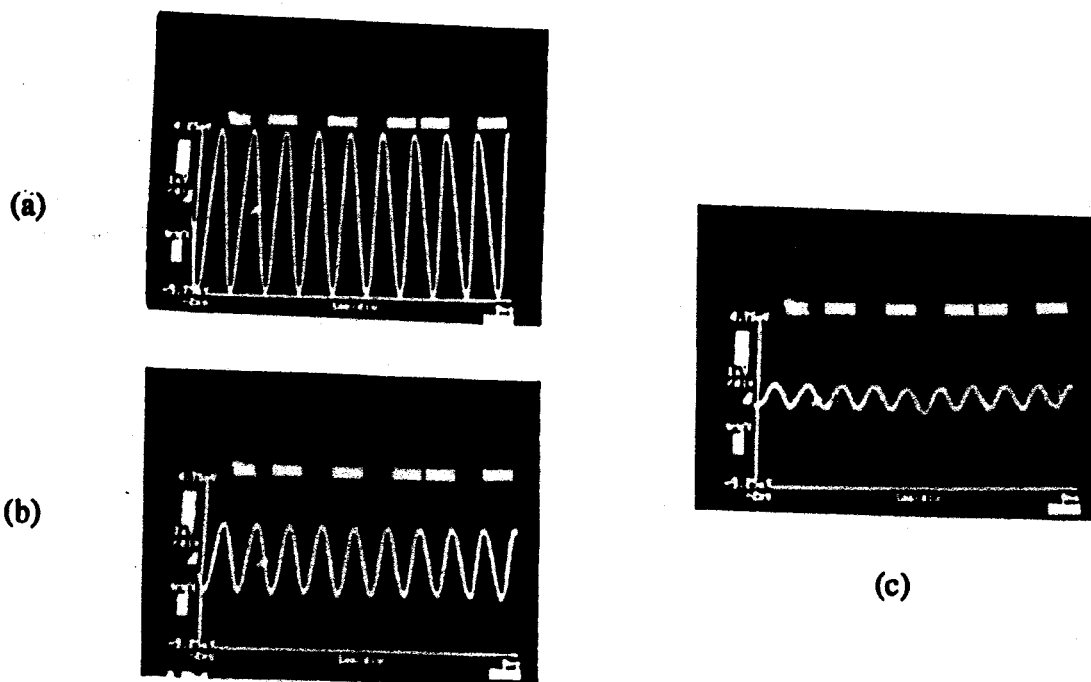


Figure 5. Input and output signals of the optical fan-out interconnect system in figure 3. (a) is the input signal, (b) is the first output fan-out and (c) is the 10th output fan-out.

Figure 6 is the plot between the measured output intensities(normalized) and the corresponding fan-outs for the 1-to-10 fan-out optical bus. The plot indicates that the intensities are not uniform for the fan-outs. New fabrication techniques are being investigated to solve this problem. The input coupling

efficiency of the device is experimentally determined to be 19.2%. The light in the optical bus is TE polarized (p-waves).

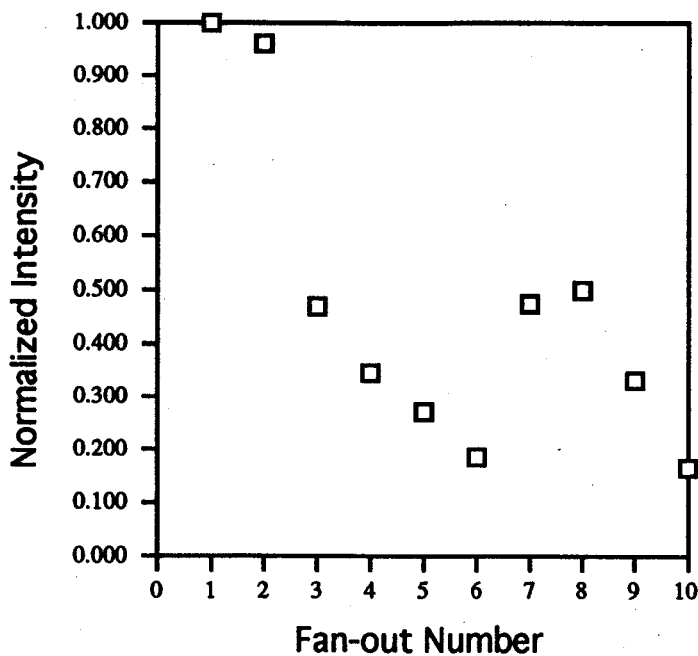


Figure. 6. Plot between the fan-outs and their corresponding intensities.

The same setup is used to determine the input angle deviation. Measurements are done for four of the fan-out beams from the optical bus. The width of the curve for any intensity is a measure of $d\theta_i$ for that intensity.

In our experiment, $d\theta_i$ is measured at 90% of the maximum intensity(normalized). A higher intensity corresponds to a smaller deviation of the incident beam, and hence the diffraction beam. The maximum deviation of the diffracted beam is limited by the active area of the detector, which is very small in our experiment. The active area radius is 100 μm , in our application. This is the reason why the calculations are done at such high intensity levels. A more detailed treatment of this concept will be provided in a following section. The next section discusses the calculation of the modulation bandwidth, using the experimental value of the angular tolerance.

4.0 Bandwidth Limitation

The wavelength tolerances of the optical bus are related to the angular tolerances through the following relation [6]:

$$d\theta_i/d\lambda = K/[4\pi n \sin(\phi - \theta_i)] \quad (1)$$

θ_i is the incident angle and ϕ is the grating slant angle, and n is the emulsion index.

where K is the magnitude of the grating vector and $K = 2\pi n \sin(45^\circ/2)/\lambda$

In our experiment, $n = 1.5$, $\phi = 45^\circ$, $\theta_i = 0^\circ$

Since all the quantities in equation 1 are known, $d\lambda$ can be calculated. The value of this wavelength deviation is determined to be 42 nm.

It is important to note that the thickness of the grating is not involved in the calculation. In order to understand this concept, consider the following equations, relating $d\lambda$ and $d\theta$ [6]:

$$d\theta[Kd \sin(\phi - \theta_i)]/2C = -d\lambda K^2 d/8\pi n C = \xi \quad (2)$$

where d is the grating thickness, $C = \cos\theta_i - K \cos\phi/\beta$, $\beta = 2\pi n/\lambda$ and ξ is the corresponding angular deviation.

From equation 2 we can obtain equation 1. Since equation 1 is a ratio, the parameters d and C cancel out. This is the reason why, the grating thickness is not a parameter of concern in this case. We substitute the angular deviation ξ into the following expression for the normalized output efficiency [6]:

$$\eta = \sin^2(v^2 + \xi^2)^{1/2} / (1 + \xi^2/v^2) \quad (3)$$

where $v = \pi n d / \lambda (C C_1)^{1/2}$ and $C_1 = \cos\theta_i$

A theoretical plot between the angular tolerance and the normalized efficiency can now be obtained. In this case, a grating thickness of 20 microns is used in the calculations. Figure 7 shows the theoretical and experimental plots between the angular misalignment and normalized intensity (efficiency). The two plots are in close agreement with one another.



Figure. 7. Change in intensity (efficiency) with angular misalignment.

For the theoretical case the normalized output efficiency is actually η^2 . The overall efficiency is the product of the efficiencies of the input coupler and the fan-out hologram. This results in a closer resemblance to the experimental data, where the incident light encounters two gratings before fan-out.

The frequency shift corresponding to this wavelength shift can be calculated according to the following first order approximation:

$$d\nu = (c/\lambda^2) d\lambda \quad (4)$$

The wavelength coverage determined by transforming the angular fluctuation to wavelength fluctuation is 42 nm, which is equivalent to 7.5 THz base bandwidth.

In high-speed applications, the active area of the detector is very small. In our application, the radius of the active area is 100 microns. Figure 8 shows how the maximum deviation in the diffracted beam is limited by the active area of the detector. In this figure, the diffracted beam traverses a radius of the active area of the detector. The beam strikes the center of the detector and moves along the radius.

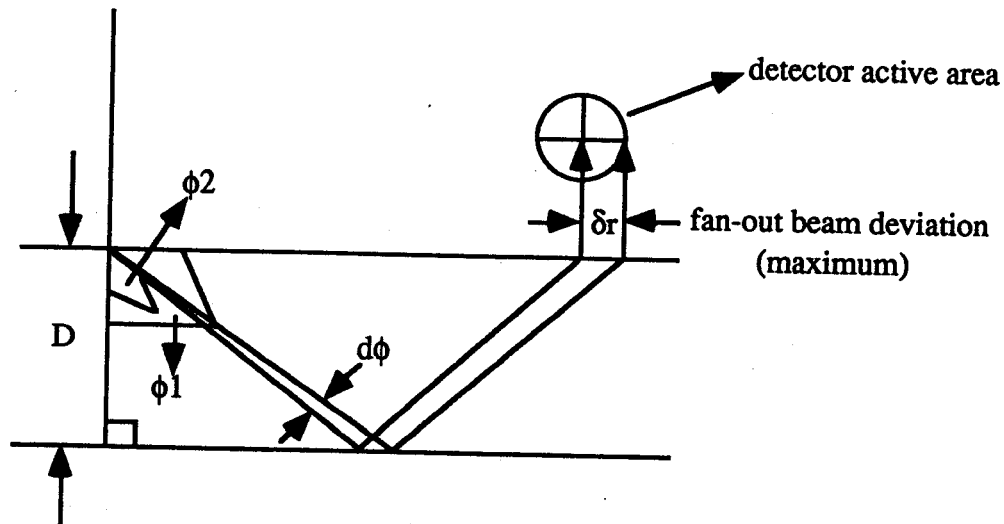


Figure 8. The active area of the detector sets the maximum limit for the deviation in the diffraction beam. The detector size limits the system performance (only one fan-out is shown).

Equation 5 is a direct result of trigonometric calculations from figure 8, which is

$$\delta r = 2DN(\tan\phi_1 - \tan\phi_2) \quad (5)$$

where δr represents the radius of the active area of the detector, which is 100 μm in our application.

$D = 3000 \mu\text{m}$ (substrate thickness), $N = 10$ (number of fan-outs).

And ϕ_1 is the input diffraction angle, which is 45 degrees in our case. From equation 5, ϕ_2 can be calculated. $\phi_1 - \phi_2$ is the maximum deviation that is possible for the detector with an active area radius of about 100 microns ($\phi_1 - \phi_2 = d\phi$).

The input angular misalignment will cause a shift in the diffraction angle. The shift in diffraction angle can be calculated using equation 7. The input angle deviation can be calculated using the following relation:

$$d\phi = -[\cos(\theta_i)/n\cos(\phi)]d\theta_i \quad (6)$$

which can be obtained by differentiating the phase-matching condition while holding the wavelength fixed. The phase matching condition is given by the following relation:

$$n\sin(\phi) = \lambda/d - \sin(\theta_i) \quad (7)$$

The input angle deviation can be calculated from equation 6. Using this value, the wavelength deviation can be calculated from equation 1. The bandwidth from these calculations is 5 nm. This clearly indicates that the detector size limits the bandwidth of the system that incorporates the bus, though the bus itself has a bandwidth, an order of magnitude higher. The frequency shift associated with this bandwidth is 890 GHz, which is still a very high value.

5.0 Conclusions

The modulation capability of a wide-band backplane 1-to-10 fan-out interconnect is determined using optical dispersion technique. The optical backplane bus is realized using a light-guiding glass in conjunction with an array of 1-D holograms. 1 Gbit/sec board-to-board interconnect through an optical backplane bus is demonstrated. The angular tolerance of the bus is 0.5° . The bandwidth coverage of the bus is 42 nm, which is determined to be corresponding to a modulation bandwidth of 7.5 THz. The bandwidth, when a small high speed detector is employed, is 5 nm. This optical backplane bus can serve as an extremely efficient interconnect in any high speed communication system. The modulation speed of the source and the response speed of the detector, pose a limitation on the system speed, rather than the optical bus itself.

6.0 References

1. Ray T Chen, Hey Lu, Daniel Robinson, Michael Wang, Gajendra Savant, and Tomasz Jansson, "Guided-Wave Planar Optical Interconnects Using Highly Multiplexed Polymer Waveguide Holograms", *J. Lightwave Tech.*, Vol. 10, No. 7, pp. 888-897, 1992.
2. M. R. Feldman, S. C. Esener, C. C. Guest, and S. H. Lee, "Comparison between optical and electrical interconnects based on power and speed considerations," *Appl. Opt.*, vol. 27, pp. 1742-1751, 1988.
3. Ray T. Chen, Suning Tang, Gajendra Savant, and Tomasz Jansson, "Compression-molded polymer based optical bus," *SPIE*, Vol. 1849, pp. 59-67, 1993.
4. Suning Tang, and Ray T. Chen, "1-to-27 highly parallel three-dimensional intra and inter-board optical interconnects," accepted for publication by *IEEE Photonics Technology Letters*.
5. Ray T. Chen, Suning Tang, Maggie M. Li, David Gerold, and Srikanth Natarajan, "1-to-12 surface normal three-dimensional optical interconnects," *Appl. Phys. Lett.*, Vol. 63, No. 20, pp. 1883-1885, 1993.
6. Herwig Kogelnik, "Coupled wave theory for thick hologram gratings," *The Bell System Technical Journal*, Vol. 48, No. 9, pp. 2909-2947, 1969.
7. Ray. T. Chen, "Polymer gelatin microstructure waveguides in conjunction with HOE for electronics and VLSI optical interconnects," *Final Report*, Contract No. DASG60-90-C-0018.